ASTRONOMY & ASTROPHYSICS
SUPPLEMENT SERIES

Astron. Astrophys. Suppl. Ser. **133**, 201–209 (1998)

Spectral classification of unidentified IRAS sources with $F_\nu(12\ \mu\mathrm{m}) \geq F_\nu(25\ \mu\mathrm{m})^\star$

K.V.K. Iyengar[1] **and D.J. MacConnell**[2]

[1] Indian Institute of Astrophysics, Bangalore 560 034, India
[2] Computer Sciences Corporation, System Sciences Division, Space Telescope Science Institute, Baltimore, Maryland, U.S.A.

Received December 4; accepted June 5, 1998

Abstract. Spectral types of a large number of unidentified IRAS Point Sources with $F_\nu(12\ \mu\mathrm{m}) \geq F_\nu(25\ \mu\mathrm{m})$ were determined; the majority are faint, oxygen-rich (M-type) or carbon-rich giant stars. The Guide Star Catalog has been used to find the photographic magnitudes of the newly classified IRAS sources with quality-3 flux densities at 12 μm in order to determine their B_j $-$[12] colour index. The dependence of this and of the IRAS indices on spectral type is determined and discussed.

The mean [12]$-$[25] colour of the M-type stars is found to increase monotonically from M3 to M6 and then levels off. Comparison of the [12]$-$[25] colours of these faint IRAS M stars with those of Bright Star Catalog M stars indicates that, at all types, the mean [12]$-$[25] index of the former group is higher than that of the latter by at least 0.2 magnitude, and this is found to be significant at the 95% confidence level. Comparison of the quality-3, mean [25]$-$[60] colours of the newly-classified, faint M stars with those of BSC stars over the same spectral type also shows the same trend. Possible reasons for this difference are discussed.

The percentage of variable sources as a function of spectral type is seen to sharply increase from a nearly constant value of about 25% for sources of spectral type M3 to M7 to a value of about 50% at M10. The mean [12]$-$[25] colours of the IRAS unidentified sources (within the limits of the errors on their mean values) appear to be rather insensitive to the degree of variability.

Key words: stars: AGB — stars: carbon — stars: late-type — stars: mass-loss — infrared: stars

Send offprint requests to: K.V.K. Iyengar

* Table 6 is only available in electronic form at the CDS via anonymous ftp to cdsarc.u-strasbg.fr (130 79 128 5) or via http://cdsweb.u-strasbg.fr/Abstract.html

1. Introduction

The Infrared Astronomical Satellite (IRAS) Point Source Catalog (PSC) contains a large number of Sources without counterparts in other astronomical catalogues. About 20% of these have $F_\nu(12\ \mu\mathrm{m}) \geq F_\nu(25\ \mu\mathrm{m})$ and lie within 7° of the southern galactic plane. Sources of this colour characteristic are expected to be mass-losing, giant stars of the M-S-C sequence having photospheric colour temperatures in the range 1500 $-$ 3000 K. Although considerable efforts have been made to identify and observe selected groups of these in other wavelength bands since the publication of the PSC in 1988, a large number of these still remain unidentified/unassociated. Many articles have appeared on the IRAS colours of particular groups of IRAS sources, and position in colour-colour diagrams has been used to classify them as either C- or O-rich stars since they preferentially populate certain "occupation zones" of the diagrams containing about 70% of the stars in each group (see e.g. Walker & Cohen 1988 and references therein).

van der Veen & Habing (1988, hereafter VH) studied the IRAS sources with circumstellar envelopes (CSE) and placed them into ten evolutionary groups based on location in the [25]$-$[60] vs. [12]$-$[25] colour-colour diagram. In their notation, the index [12]$-$[25] is defined as $2.5 \times [\log(F_\nu(25)/F_\nu(12))]$ and similarly for [25]$-$[60] where the $F_\nu(\lambda)'s$ are the IRAS flux densities at 12, 25, and 60 μm uncorrected for colour dependence. Except when we discuss the [25]$-$[60] vs. [12]$-$[25] colour-colour diagram presented in Fig. 13, throughout the rest of the text, tables and figures (unless otherwise specifically stated) the IRAS magnitudes referred to by us are defined as $[\lambda] = -2.5 \times [\log(F_\nu(\lambda)/F_{\nu 0}(\lambda))]$ where $[\lambda]$ is the IRAS magnitude of the source at the wavelength λ in μm, $F_\nu(\lambda)$, is the flux density in Jy at wavelength λ, and $F_{\nu 0}(\lambda)$ its zero magnitude flux density in Jy at wavelength λ as given in the IRAS PSC Explanatory Supplement (IRAS PSC, 1988). Stars with O-rich envelopes form a sequence in the [25]$-$[60] vs. [12]$-$[25] colour-colour

diagram. This has been interpreted as 1) due to evolution of mass loss rate (Olnon et al. 1984; Bedijn 1987; van der Veen & Habing 1988); 2) a sequence of increasing initial mass (Epchtein et al. 1990); and 3) due to the combined effects of increasing mass-loss rate and increasing initial stellar mass (Likkel 1990). VH showed that the evolutionary track of most of these stars in the [25]−[60] vs. [12]−[25] colour-colour diagram is a single-valued function of [12]−[25] colour. This track passes through regions I, II, IIIa, IIIb and IV of VH; see Fig. 13. There are, however, other stars with CSE that populate a much wider area of this colour-colour diagram. Some are those that have cooler envelopes due to higher emissivity of carbon dust in their envelopes. Thus, it has been claimed that the VH diagram serves as a useful tool for obtaining preliminary information on the evolutionary status of stars with CSE.

A major fraction of the unidentified sources of this study do not have best-quality (IRAS quality-3) flux density data at wavelengths longward of 12 μm. Sources with $F_\nu(12\ \mu\text{m}) \geq F_\nu(25\ \mu\text{m})$ are likely to emit fairly strongly in the optical-infrared region even if faint (as is expected of most of the unidentified sources). As spectral type data on these sources provide valuable information for an evolutionary classification of these sources, DJM carried out spectral classification of these sources using objective-prism plates collected by him. These plates were limited to the galactic latitude belt of $\pm 7^\circ$. We present here results on approximately 10 000 IRAS unidentified sources in the R.A. zone $5^\text{h}17^\text{m}$ to $12^\text{h}06^\text{m}$.

2. Observation and classification of unidentified sources

It would be unthinkably inefficient to obtain the individual spectra of the unidentified IRAS sources (in view of their extremely large number) and to classify them. On the other hand, objective-prism plates taken with a Schmidt Camera enable one to classify the spectra of all objects covered in the field in a single exposure. The wavelength region most appropriate for obtaining spectral information on unidentified IRAS sources is the photographic infrared. In this region, between 0.7 μm and 0.9 μm, strong diatomic bands dominate the spectra of cool stars: TiO and VO in the M stars, CN in the cooler (N-type) carbon stars, and LaO in the pure S stars. These features can be distinguished readily in objective prism spectra at dispersions as low as 3400 Å mm^{-1} at the telluric A-band and have been used to discover and classify cool stars since Nassau and colleagues pioneered in the use of Kodak I-N emulsion with objective prisms in the late 1940's (Nassau & van Albada 1949).

DJM (MacConnell 1992) collected I-N spectrum plates of dispersion 3400 Å mm^{-1} with the Curtis Schmidt Camera at CTIO; the deepest reach $I \sim 13.5$. The plate scale is $96\farcs6$ mm^{-1}, and each covers $5^\circ \times 5^\circ$. They cover the galactic latitude belt $\pm 7^\circ$ along the full southern galactic plane. In the years 1986-92, DJM classified about 14 200 IRAS sources (identified as well as unidentified) in the R.A range $5^\text{h}17^\text{m}$ to 14^h with $F_\nu(12\ \mu\text{m}) \geq F_\nu(25\ \mu\text{m})$ falling in the area of the available plates. These constitute nearly 40% of all IRAS PSC sources of this type. The majority of these IRAS sources have cool stellar photospheres in the visible region, and the above colour criterion ensures that their CSE are warmer than 300 K. Stars earlier than type M3 have TiO bands too weak to be seen on these plates and so cannot be classified.

Table 1. Statistics on the classification of IRAS Sources with $F_\nu(12\ \mu\text{m}) > F_\nu(25\ \mu\text{m})$

Type	%	Type	%
Earlier than M3:	16	Carbon:	13
M3 or M4:	12	S or S?:	2
M5 or M6:	16	M4 redd: or s?:	1
M7 or M8:	23	Very faint:	3
M9 or M10:	8	Blank field:	6

The plates were illuminated at a light table and examined at a magnification of 12X with a binocular microscope. Overlay plots to the plate scale and at the plate centers were generated for all plates at IPAC. Figure 1 shows a reduced-scale version of a plate on the appropriate IRAS plot. Stars from the SAO Catalog were also plotted to ensure the registration of plate with plot; small crosses denote positions of SAO stars. There was seldom any doubt as to which object on the plate corresponded to a given IRAS source even in the crowded galactic plane areas. The classifications and other data were stored on a microcomputer running a commercial program. Positions of the IRAS sources were measured with an $x - y$ digitizer, and the measures were converted to equatorial co-ordinates using a specialized program on the PC which wrote the IRAS Name of the source into a database record and paused for entry of the classification and other data. These classifications are on file with the Astronomical Data Center (ADC) at the Goddard Space Flight Center, and most are contained in Version 2.1 of the IRAS PSC where they are designated as Catalog # 43. The sources classified in this way may be broken down into 10 groups, and the statistics based on a sample of 10 500 classifications are listed in Table 1. The uncertainty in a type is ± 1 subclass.

We examine here the data of only the unidentified IRAS sources which could be classified as O-rich stars (spectral type M) i) to search for correlations between spectral types and IRAS colours, and ii) to determine distributions of the various spectral classes in the two-colour diagrams.

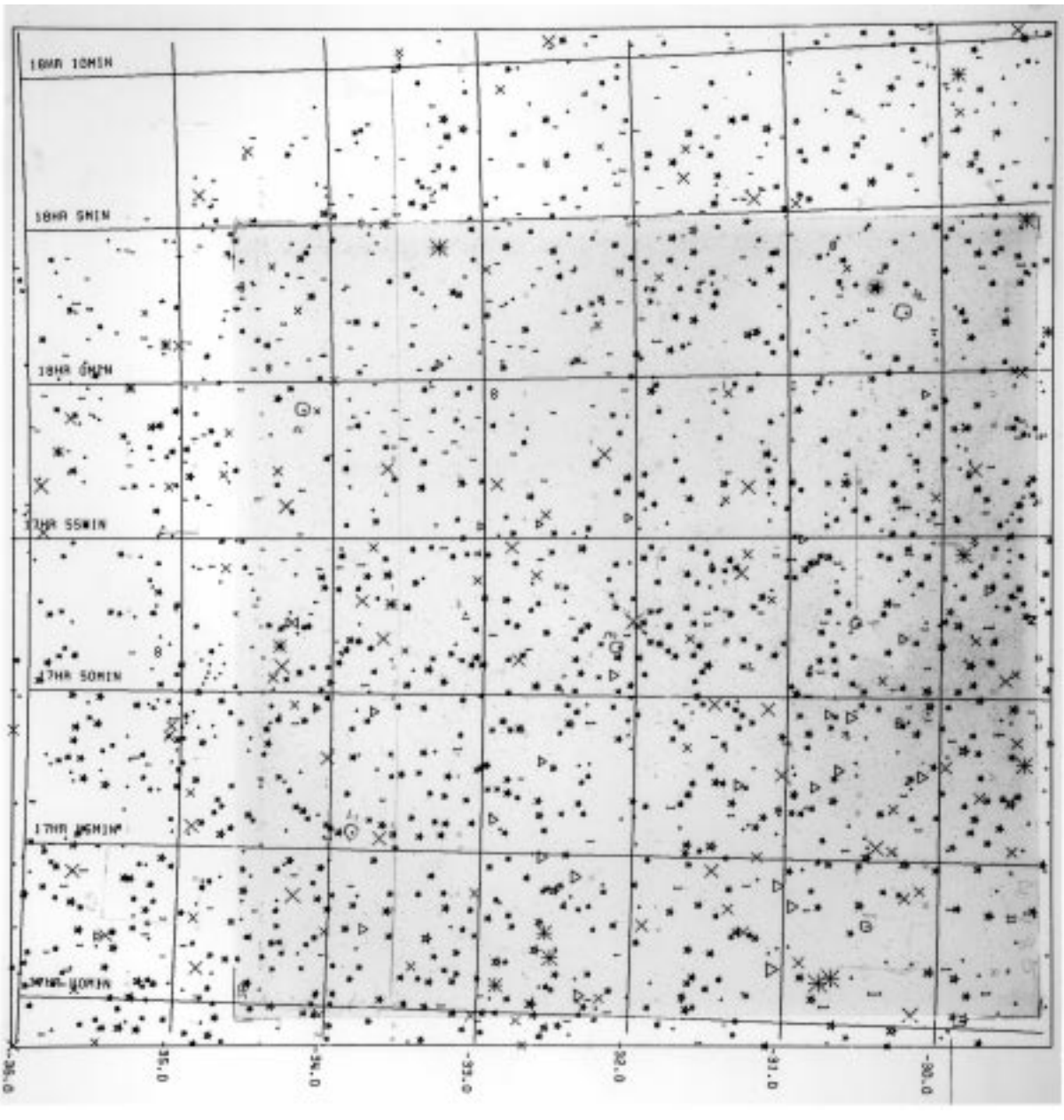

Fig. 1. Reduced-scale version of a I-N objective prism spectrum plate obtained at a dispersion of 3400 Å mm^{-1} with the Curtis Schmidt Camera at CTIO, Chile. The deepest plates reach $I \sim 13.5$. Each plate covers $5^\circ \times 5^\circ$. The plate scale is $96''.6$ mm^{-1}. The different symbols on the photographic print refer to IRAS sources with $F_\nu(12\ \mu m) \geq F\nu(25\ \mu m)$. The size of the symbol is proportional to $F_\nu(12\ \mu m)$. These symbols refer to sources as listed below: 1 = 1000, star = 1100, x = 1110, $*$ = 1111, triangle = 1101, x with bar on top = 1010, x with bar top/bottom = 1011, infinity = 1001. The four numbers on the right of the sign "=" refer in the order to the flux density of these sources at 12, 25, 60 and 100 μm respectively, where "0" means flux density is below the detection threshold and "1" means flux density is above it

3. Analysis of data and discussion

We discuss the unidentified sources for which definite spectral type assignments have been made by DJM under the categories i) sources for which quality-3 flux density data are available at only 12 μm, ii) sources for which quality-3 flux density data are available at both 12 and 25 μm, and iii) sources for which quality-3 flux density data are available at 12, 25, and 60 μm.

3.1. B_j–[12] colours of unidentified IRAS sources with quality-3 flux density data at only 12 μm

KVKI has carried out a search of the Guide Star Catalog (GSC Version 1) to obtain B_j magnitudes for the unidentified IRAS sources having quality-3 flux density data at only 12 μm (flux density upper limits in the other three bands) and having M-type spectral assignments by DJM. B_j is the magnitude determined from the UK-SERC

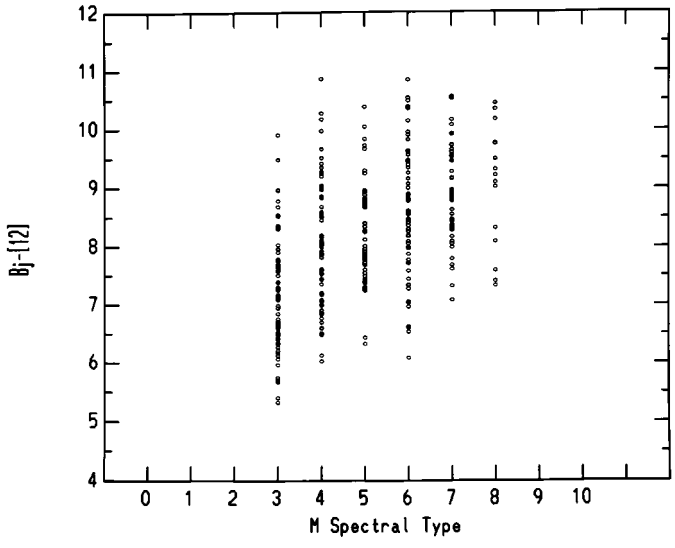

Fig. 2. B_j–[12] colour vs. spectral type of unidentified IRAS sources with best-quality flux density data at only 12 μm (which could be associated with optical counterparts) on the SERC plates by searching the Guide Star Catalog (Version 1). The optical object (when it was the only one) on the SERC plates within a circle of radius 15″ from the IRAS source position was considered as its optical counterpart. The B_j magnitudes are from GSC Version 1

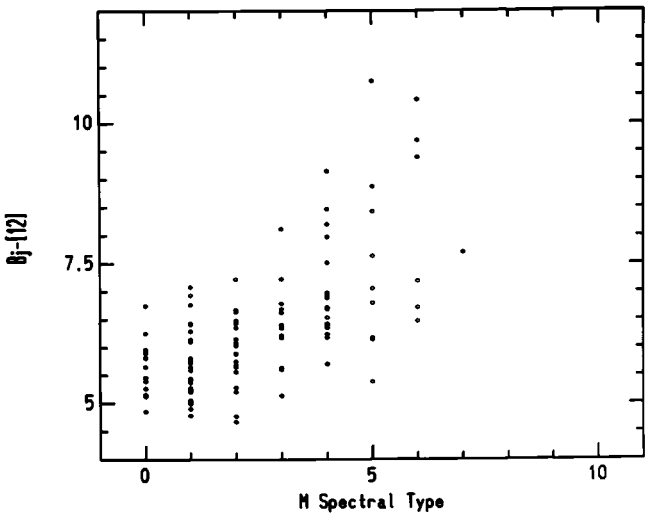

Fig. 3. Similar data as in Fig. 2 for BSC M giants. However, the BSC giants have IRAS quality-3 flux density data in the three bands 12, 25, and 60 μm unlike the IRAS unidentified sources with which they are being compared

Schmidt IIIa-J plates behind a GG 395 filter; the plates are primarily of fields south of the celestial equator. This subset of the unidentified IRAS sources is very likely to be characterised by extremely thin dust shells as their emission at 25 μm and 60 μm is below the IRAS detection threshold.

This search for optical counterparts has been restricted to the sources (numbering about 1 075) lying in the 1950 R.A. range 5^h18^m to 9^h30^m and resulted in 320 classified IRAS sources meeting the above flux criterion for which B_j magnitudes are available. The star (when it is the only one) lying within 15″ of the IRAS source position has been taken as the optical counterpart of the source.

Figure 2 presents B_j–[12] colours as a function of spectral type for this group, and Fig. 3 presents similar data for southern BSC M giants. All these stars are of late spectral type, and it is well known that many late M stars are variable in light and spectrum and thus spectral types and the optical and infrared magnitudes will depend on the phase at which they are observed. We point out that no IRAS variability data are available to study the variability of these sources as a function of spectral type since they are detected with quality-3 flux densities at only 12 μm and the requirement for a source to be listed as variable in the IRAS PSC is that the changes in the flux density at 12 μm and 25 μm be correlated. However, IRAS variability data are available (from IRAS PSC) for the BSC stars with which the colours of the IRAS unidentified sources have been compared. The incidence of variability of the BSC stars is quite low and does not show any definite dependence on spectral type. It is necessary to stress that the spectral type assignments of the sources discussed in this study are based on observations at epochs different from those for which the optical (from Sky Surveys) and the infrared magnitudes (from IRAS observations of 1983) are available. The differences in the epochs are expected to result in an enhancement of the scatter in the estimated colours (due to variability alone) as a function of spectral type. An additional source of scatter in the colours is due to differing amounts of interstellar extinction at B_j since interstellar extinction is near zero beyond 10 μm. The inclined lower bound to the points in these figures is presumably the locus of unreddened M giants with the thinnest CSE. The data on the mean B_j–[12] colours as a function of spectral type for the unidentified IRAS sources and BSC M giants are presented in Table 2. The entries are as follow: Column (i) is the spectral subtype of the sources and in columns (ii) - (iv) and in (v) - (vii) are the number of sources of a particular spectral type, their mean B_j–[12] colour, and root mean square (rms) deviation in the value of the mean colour for the BSC stars and the unidentified IRAS sources, respectively. In Fig. 4 the mean values are given, and there is a noteworthy difference in the mean B_j–[12] colours in the region of spectral type overlap albeit there are large statistical errors on the mean colours of the two groups. Kolmogorov-Smirnov (K-S) and Wilcoxon two-sided tests show that the two samples are not from the same population at the 95% confidence level. The difference is, no doubt, due to higher values of extinction toward the more distant, unidentified IRAS sources than toward the more local BSC M giants. Cohen et al. (1987) in their Fig. 4 presented V–[12] vs. spectral type for the BSC giants, and the trend for the M stars is

Table 2. Mean B_j–[12] colours of M-type BSC stars and IRAS unidentified sources

	BSC Stars			IRAS unidentified Sources		
Sp. Subtype	No.	Mean	rms deviation	No.	Mean	rms deviation
M0	14	5.63	0.50			
M1	28	5.57	0.84			
M2	23	5.94	0.61			
M3	13	6.41	0.75	77	7.21	0.98
M4	19	7.00	0.88	64	8.06	1.09
M5	8	7.06	1.19	49	8.20	0.88
M6	6	8.31	1.72	61	8.53	1.13
M7				53	8.88	0.83
M8				15	9.03	1.05
M9						
M10						

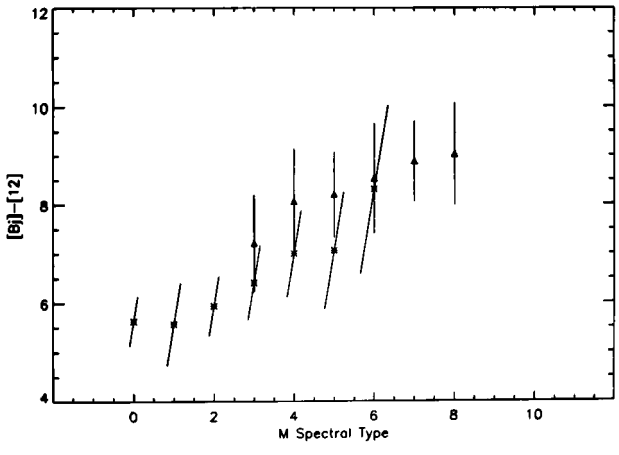

Fig. 4. Mean B_j–[12] colours of IRAS unidentified sources and of BSC giants as a function of M spectral type. The symbols "delta" and "*" refer to IRAS unidentified sources and BSC giants, respectively. The error bars shown on the data points correspond to the rms deviations of the colours from their mean values. The error bars on the mean colours of the BSC stars are shown slanted to avoid overlaps

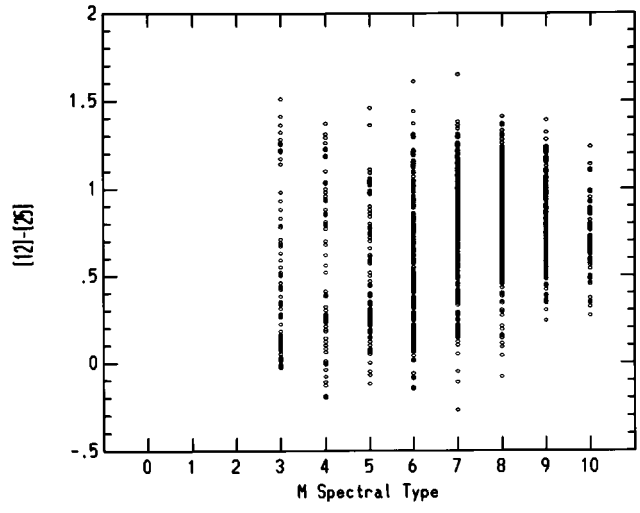

Fig. 5. [12]−[25] colour of IRAS unidentified sources which have best-quality flux density data vs. their M spectral type

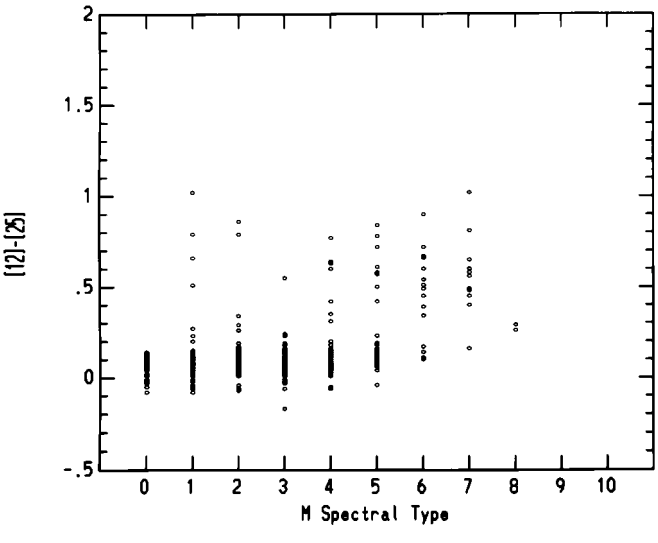

Fig. 6. Similar data as in Fig. 5 for BSC M giants

similar to ours and is what is expected given the difference in magnitude systems.

3.2. [12]−[25] colours of unidentified sources detected at both 12 and 25 μm

We have determined the [12]−[25] colours as a function of spectral type for all unidentified IRAS sources of quality-3 in this study, and these are presented in Fig. 5 for ∼1890 IRAS sources. One sees from the figure that there is an increase in [12]−[25] colour towards later spectral types and a large spread at each spectral type. We have used these data to obtain the mean [12]−[25] colours of these sources as a function of spectral type. To compare these data with those of M giants in the BSC, we have plotted in Fig. 6 the [12]−[25] colours of the BSC stars for which IRAS photometric data of quality-3 are available in these bands. In Table 3 we compare the mean [12]−[25] colours of BSC stars with those of unidentified IRAS sources. The entries in Table 3 are as those in Table 2 except that the colour referred to here is [12]−[25] instead of B_j–[12]. The dependences of the mean [12]−[25] colours of these two types of sources as a function of spectral type are presented in Fig. 7. It is seen that the mean [12]−[25] colours of the IRAS sources are consistently higher than those of BSC stars as was the case in Fig. 4 although the colours (in the region of overlap) are within the statistical errors. K-S and Wilcoxon tests again indicate that the two samples are from different populations at the 95% confidence level. In Fig. 4, the difference was explained as due to greater interstellar extinction for the fainter, unidentified IRAS sources, whereas the difference between the two groups cannot be explained that way for the data in Fig. 7 since interstellar extinction is nearly negligible at both 12 and 25 μm. The difference may be a selection effect due to

Table 3. Mean [12]−[25] colours of M-type BSC stars and IRAS unidentified sources

	BSC Stars			IRAS unidentified Sources		
Sp. Subtype	No.	Mean	rms deviation	No.	Mean	rms deviation
M0	61	0.05	0.05			
M1	85	0.10	0.16			
M2	105	0.09	0.12			
M3	84	0.08	0.08	69	0.49	0.44
M4	72	0.13	0.15	76	0.55	0.46
M5	37	0.24	0.25	106	0.46	0.34
M6	17	0.42	0.25	317	0.62	0.33
M7	12	0.56	0.21	485	0.77	0.28
M8				501	0.83	0.23
M9				258	0.79	0.21
M10				78	0.71	0.19

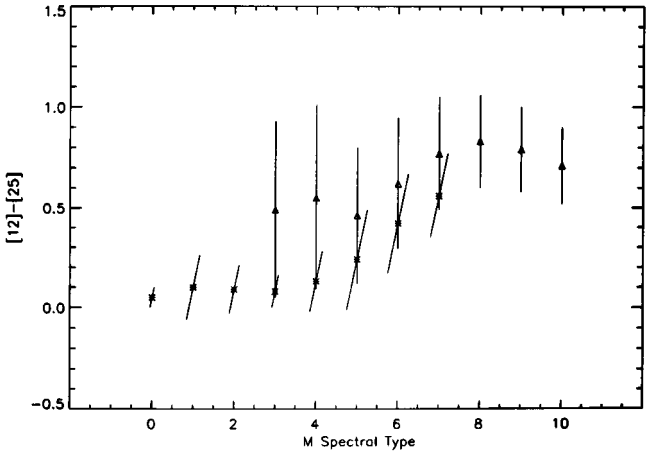

Fig. 7. Mean [12]−[25] colours of IRAS unidentified sources and BSC giants vs. M spectral type. The symbols "delta" and "*" have the same meanings as in Fig. 4. The error bars shown on the data points correspond to the rms deviations of the colours from their mean values. The error bars on the mean colours of the BSC stars are shown slanted to avoid overlaps

the difference in the volumes sampled around the faint, more distant IRAS sources with thick CSE compared to the local BSC M stars with almost dust-free photospheres.

An index of the variability of the source, listed as IVAR (expressed as a percentage) is available from IRAS PSC for 1890 unidentified IRAS sources which have quality-3 flux densities at both 12 μm and 25 μm and spectral type assignments. Of these 1334 have a variability index IVAR < 25 and the remaining 556 have a variability index IVAR > 25. The value of this index is based on correlated observations of IRAS sources simultaneously in the two spectral bands, 12 μm and at 25 μm. We present in Table 4 the distribution of these unidentified IRAS sources with [12]−[25] colours in two bins of IVAR. It will be noticed that about 25% of the sources with spectral types ranging from M3 to M7 have IVAR > 25 but the percentage of sources with IVAR > 25 increases sharply from spectral type M8 onwards to a value of about 55% at spectral type M10. This is however, not surprising as M stars of later spectral type are known to have a higher incidence of variability. We present in Fig. 8 the [12]−[25] colour vs. M spectral type for these sources whose IRAS variability index IVAR is < 25 and, in Fig. 9, [12]−[25] colour for sources whose variability index IVAR is > 25. The mean [12]−[25] colours of these sources as a function of their spectral type appear not to depend on the variability index (within the limits of errors on these mean colours). K-S and Wilcoxon two-sided tests indicate that there is about 90% chance that the points in Figs. 8 and 9 (are from the same population). We therfore conclude that variability has minimal effect on the distribution of points in Fig. 5.

We point out that, the mean [12]−[25] colours of the northern IRAS sources classified by Stephenson (1986) for M6−M9, fall within 0.1 mag of ours which adds confidence to our conclusion.

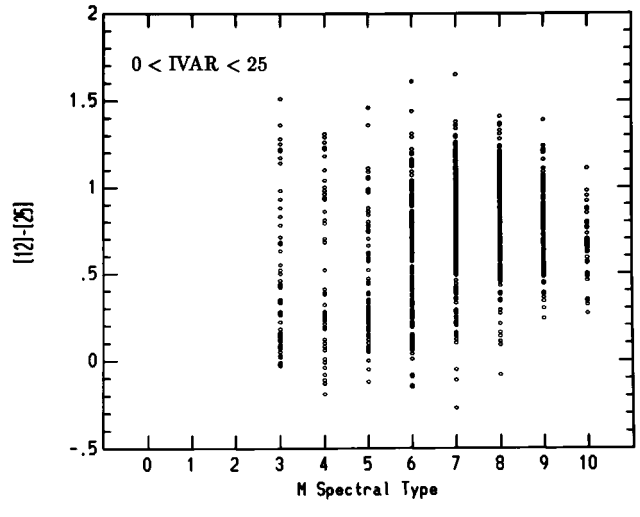

Fig. 8. [12]−[25] colour vs. M spectral type of unidentified IRAS sources with quality-3 flux densities at both 12 μm and 25 μm and whose variability index IVAR is < 25

3.3. [25]−[60] colours vs. spectral type of unidentified sources

The [25]−[60] colours of IRAS unidentified sources and BSC M giants as a function of spectral type are presented in Figs. 10 and 11, respectively. The mean [25]−[60] colours of the two groups are presented in Fig. 12, and the mean data are given in Table 5. The entries in Table 5 are as those in Table 2 except that the colour referred to here is [25]−[60] instead of B_j–[12] as in the case of Table 2. The mean [25]−[60] colours of unidentified IRAS sources are seen to be always higher than those of BSC stars in the region of overlap of spectral types as in the case of B_j–[12] and [12]−[25] colours. The K-S and Wilcoxon tests show

Table 4. No. distribution of unidentified IRAS sources with [12]–[25] colours in two bins of IRAS variability index (IVAR)

Spectral type	No. with IVAR < 25	No. with IVAR > 25	Percentage of sources with IVAR > 25
M3	55	14	20
M4	56	20	26
M5	83	23	22
M6	235	82	26
M7	368	117	24
M8	354	147	29
M9	147	111	43
M10	36	42	54
M3-M10	1334	556	29

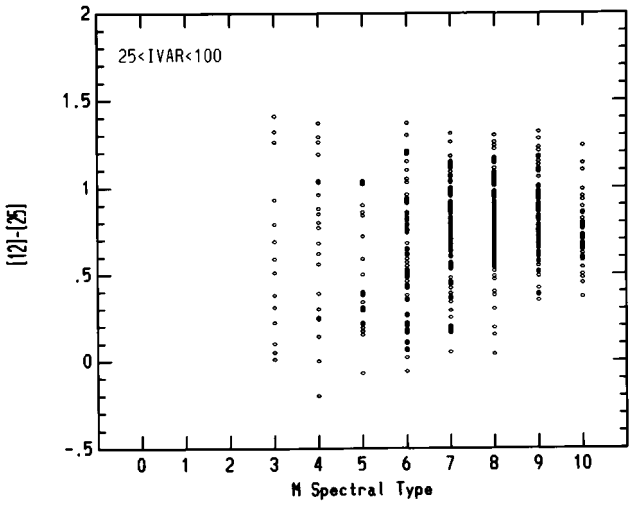

Fig. 9. [12]−[25] colour vs. M spectral type of unidentified IRAS sources with quality-3 flux densities at both 12 μm and 25 μm and whose variability index IVAR is > 25

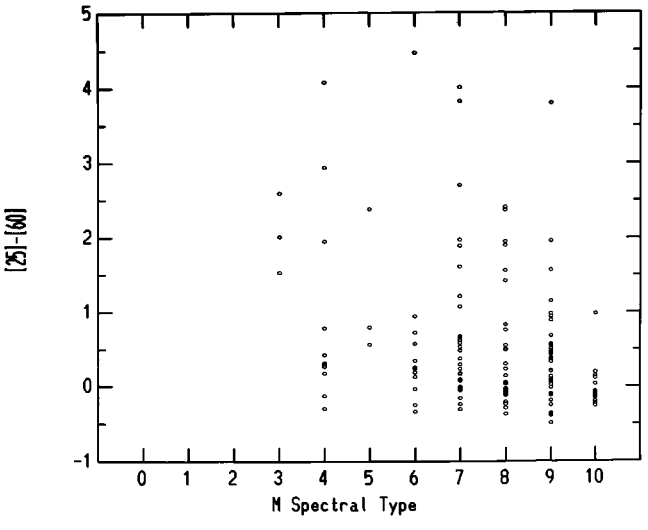

Fig. 10. [25]−[60] colour of IRAS unidentified sources which have best-quality flux density data in both these wavelength bands vs. their spectral type

that the IRAS sources are different from the BSC sources at the 95% confidence level.

4. [25]−[60] vs. [12]−[25] colour-colour diagram of unidentified sources

The unidentified IRAS sources for which quality-3 flux density data are available from the IRAS PSC in the 12, 25, and 60 μm bands and for which M spectral assignments by DJM were available were used to generate the [25]−[60] vs. [12]−[25] colour-colour diagram which is presented in Fig. 13; there are 156 sources in this category. A large number of these sources can no longer be called unidentified as they have been observed in other wavelength bands, although not always with positive detection. Thirty-eight of these have been observed in the near-IR bands by Guglielmo et al. (1993) and some of these have been classified by them as O-rich stars. Sources 06528−1405, 07231−0300, 07528−3928, 08043−3709, 09519−6007, and

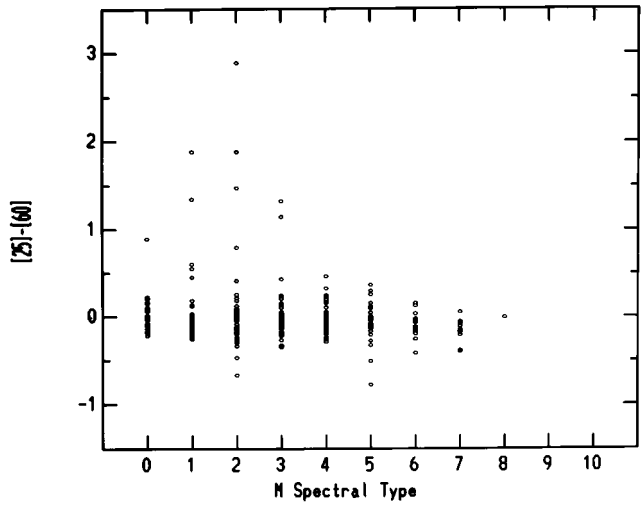

Fig. 11. Similar data as in Fig. 10 for BSC giants

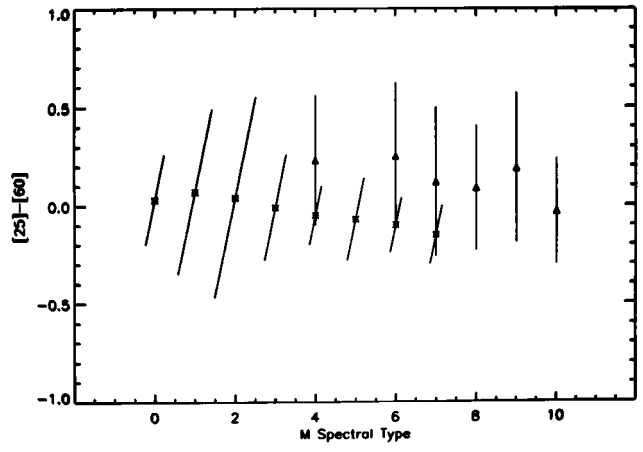

Fig. 12. Mean [25]−[60] colours of unidentified IRAS sources and BSC giants vs. M spectral type. The symbols "delta" and "*" have the same meanings as in Fig. 4. A large number of sources have [25]−[60] colours which deviate by a very large margin from their mean values (see Fig. 10). The mean [25]−[60] colours (shown in this figure) of the IRAS unidentified sources are therefore limited to only those sources whose [25]−[60] colour is ≤ 1.0. Mean colours of stars with spectral types numbering ≤ 5 are not shown in the figure as they are not statistically significant. The error bars shown on the data points correspond to the rms deviations of the colours from their mean values. The error bars on the mean colours of the BSC stars are shown slanted to avoid overlaps

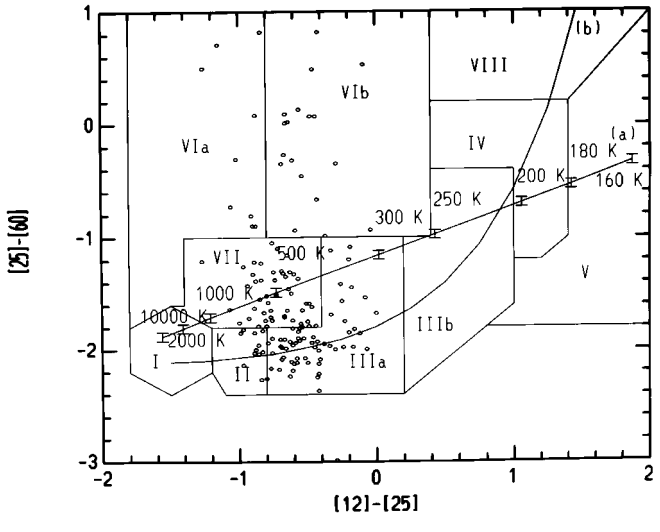

Fig. 13. Diagram showing the regions in the colour-colour plot of [25]−[60] vs. [12]−[25] that separate different types of stars with CSE (adopted from van der Veen & Habing 1988; VH). The colours [25]−[60] and [12]−[25] are as defined by VH. The evolutionary track is indicated by the curve "b", $([25]-[60]) = -2.15 + 0.35 \times e^{1.5([12]-[25])}$ which represents the observed colours very well for $-1.1 < ([12]-[25]) < 1.3$. The line "a" shows the loci of black bodies with temperatures ranging from 10 000 K to 160 K with specific values shown at the vertical bars on the line. The circles refer to the positions of the IRAS unidentified sources of M spectral type

Table 5. Mean [25]−[60] colours of M-type BSC stars and IRAS unidentified sources

	BSC Stars			IRAS unidentified Sources		
Sp. Subtype	No.	Mean	rms deviation	No.	Mean	rms deviation
M0	22	0.03	0.23			
M1	37	0.07	0.42			
M2	65	0.04	0.51			
M3	64	−0.01	0.27			
M4	52	−0.05	0.15	8	0.23	0.33
M5	33	−0.07	0.21			
M6	16	−0.10	0.14	12	0.25	0.37
M7	11	−0.15	0.15	27	0.12	0.38
M8				25	0.09	0.32
M9				35	0.19	0.38
M10				20	−0.03	0.27

10360−5633 have been identified by Kwok et al. (1997) as the variable stars GR CMa, V686 Mon, AO Pup, OY Pup, V363 Car, and CoD-56 3464, respectively. The data on these sources are presented in Table 6, in which the entries in Cols. 1-11 are: IRAS Name of the source, galactic longitude and latitude, spectral type of the source (from DJM), the IRAS magnitudes at 12, 25, and 60 μm and the $([12]-[25])_{VH}$ and $([25]-[60])_{VH}$ where these colours are as defined by VH (refer to text), IVAR and LRS type from the IRAS PSC, respectively. The superscripts on the IRAS Name of the source in Col. 1 cite references to available literature on these sources. According to VH, the colour-colour diagram provides information on the evolutionary stage of the sources.

The IRAS sources of this study occupy the regions II, IIIa, VIa, VIb and VII (see VH). Sources in region II are classified by VH as variable stars with "young", O-rich CSE, those in region IIIa as stars with more evolved, O-rich CSE, those in region VIa as non-variable stars with relatively cold dust shells at large distances from the star (of which a significant part are C-rich), IRAS sources in region VIb are classified as variable stars with relatively hot dust close to the star and cooler dust at large distances (some of which are known to be O-rich), and those in region VII as variable stars with more evolved, C-rich CSE. However, over 50 sources, i.e., about 1/3 of those plotted in Fig. 13, fall in region VIa and VII but have M-star photospheres as per the objective-prism classifications. As is well known due to the overlap in the colours of different spectral types in certain regions of the colour-colour diagram, it is not possible to classify the sources unambiguously as either O-rich or C-rich sources. This is in conformity with our findings based on spectral type data.

A parameter study of the spectral evolution of a typical post-AGB star with particular emphasis on the evolution of infrared colours carried out by van Hoof et al. (1997) shows that the variations of the several model parameters (considered by them) results in a variety of different paths in the IRAS colour-colour diagram. As a

consequence of this, the same location in the IRAS colour-colour diagram can be occupied by objects with an entirely different evolutionary past. They therefore conclude that the location in the IRAS colour-colour diagram cannot a-priori give a unique determination of the evolutionary status of an object. This finding is in consonance with our own findings also.

5. Summary

Spectral-type assignments have been made for more than 14 000 IRAS sources which are primarily unidentified in the PSC and which have $F_\nu(12\ \mu\mathrm{m}) \geq F_\nu(25\ \mu\mathrm{m})$. A large number of them are either O-rich (M-type) or C-rich (C-type) stars. The mean B_j–[12], [12]−[25], and [25]−[60] colours of a sample of the M stars (from the 14 000 IRAS sources referred to above) have been obtained and compared with those of corresponding BSC M giants. The classification of these sources would not have been possible on the basis of their IRAS colours alone as most of them are detected with best-quality flux densities at only 12 μm. The mean colours of the unidentified sources are higher than those of BSC giants of the same spectral type implying that the more distant IRAS sources have thicker CSE. A plot of the [25]−[60] colours vs. [12]−[25] colours (as in VH) indicates that 1/3 of the sources which are likely to be classified as carbon stars on the basis of their location in the VH diagram are found to be of M spectral type as judged from their spectra. The spectral classification of the faint, unidentified sources discussed in this study therefore constitutes an important contribution to the available information on these galactic IRAS sources.

Acknowledgements. KVKI thanks the Director of the Indian Institute of Astrophysics (IIA) for kindly providing him the facilities of IIA while this work was being carried out. He also thanks the Smithsonian Institution, Washington DC, U.S.A. for the award of a Short-Term Visiting Appointment (and also for a short extension of this appointment) to work at the Harvard-Smithsonian Center for Astrophysics, Cambridge, Mass, U.S.A. where a major part of this work was carried out. He thanks Dr. G.G. Fazio for his kind hospitality and fruitful discussions. He also thanks the Research Programs Office of the Space Telescope Science Institute (STScI), Baltimore, MD, U.S.A. for providing financial assistance to enable him to visit DJM for discussions related to this work. DJM thanks the STScI for salary support during the visit of KVKI and during analysis of this material. We thank Profs. H. Bhatt and M. Parthasarathy (both of IIA) for several useful discussions and Dr. C. Barnbaum for a careful reading of the manuscript. We also thank Dr. van der Veen, (the referee of this paper) for several useful comments and suggestions which helped to improve the manuscript. STScI is operated by the Association of Universities for Research in Astronomy, Inc., under NASA contract NAS5-26555. DJM's classification work was supported by the NASA Astrophysics Data Program under JPL Contracts 766490 and 957272.

References

Allen L.E., Kleinmann S.G., Weinberg M.D., 1993, ApJ 411, 188
Bedijn P.J., 1987, A&A 186, 136
Cohen M., Deborah E., Schwartz D.E., Chokshi A., Walker R.G., 1987, AJ 93, 1199
Epchtein N., Le Bertre T., Lepine J.R.D., 1990, A&A 227, 82
Fouque P., Le Bertre T., Epchtein N., et al., 1992, A&AS 93, 151
Guglielmo F., Epchtein N., Le Bertre T., et al., 1993, A&AS 99, 31
Haikala L.K., Nyman L.-A., Forrstroem V., 1994, A&AS 103, 107
Hashimoto O., 1994, A&AS 107, 445
IRAS Point Source catalog Version 2; 1988. Joint IRAS Science Working group, washington, D.C., U.S. Government Printing Office, PSC
Jiang B.W., Deguchi SW., Yamamura I., et al., 1996, ApJS 106, 463
Kwok S., Volk K., Bidelman W.P., 1997, ApJS 112, 557
Lepine J.R.D., Ortiz R., Epchtein N., 1995, A&A 299, 453
Lewis B.M., Eder J., Terzian Y., 1990, ApJ 362, 634
Likkel L., 1990, in: From Miras to Planetary Nebulae: Which path for Stellar Evolution, Menessier M.O., Omont A. (eds). Éditions Frontières, p. 258
Olnon F.M., Baud B., Habing H.J., et al., 1984, ApJ 278, L41
Olnon F.M., Raimond E., IRAS Science Team. IRAS Catalogues and Atlases - Atlas of Low Resolution Spectra 1986, A&AS 65, 607
MacConnell D.J., Wing, R.F., Costa, E., 1992, AJ 104, 821
Nassau J.J., van Albada B.G., 1949, ApJ 109, 391
Sivagananm P., Braz M.A., Le Squeren A.M., et al., 1990, A&A 233, 112
Stephenson C.B., 1986, ApJ 301, 927
te Lintel Hekkert P., Caswell J.L., Habing H.J., et al., 1991, A&AS 90, 327
van der Veen V.E.C.J., Habing H.J., 1988, A&A 194, 125
van Hoof P.A.M., Oudmaijer R.D., Waters L.B.F.M., 1997, MNRAS 289, 371
Walker J.H., Cohen M., 1988, AJ 95, 1801
Volk K., Kwok S., Stencel R.E., Brugel E., 1991, ApJS 77, 607